PLEASE CITE THIS ARTICLE AS DOI: 10.1063/5.0171213

A broadband pulse amplifier for Joule heating experiments in diamond anvil cells

- Zachary M. Geballe, Joseph Lai, and Michael J. Walter 2
- Earth and Planets Laboratory, Carnegie Institution for Science, Washington, 3
- DC 20015 4

7

9

10

11

12

13

14

15

16

17

18

19

20

21

- (The author to whom correspondence may be addressed: zgeballe@carnegiescience.edu) 5
- (Dated: 27 March 2024) 6
 - Decades of measurements of the thermophysical properties of hot metals show that pulsed Joule heating is an effective method to heat solid and liquid metals that are chemically reactive or difficult to contain. In order to extend such measurements to 100s of GPa pressure, pulsed heating methods were recently integrated with diamond anvil cells. The recent design used a low-side switch and active electrical sensing equipment that was prone to damage and measurement error. Here, we report the design and characterization of new electronics that use a high-side switch and robust, passive electrical sensing equipment. The new pulse amplifier can heat ~ 5 to 50 μ m-diameter metal wires to 1000s of kelvin at 10s to 100s of GPa using diamond anvil cells. Pulse durations and peak currents can each be varied over 3 orders of magnitude, from 5 μ s to 10 ms and from 0.2 to 200 A. The pulse amplifier is integrated with a current probe. Two voltage probes attached to the body of a diamond anvil cell are used to measure voltage in a four point probe geometry. The accuracy of four point probe resistance measurements for a dummy sample with $0.1~\Omega$ resistance are typically better than 5% at all times from 2 μ s to 10 ms after the beginning of the pulse.

PLEASE CITE THIS ARTICLE AS DOI: 10.1063/5.0171213

40

41

42

43

44

45

46

47

48

49

2 I. INTRODUCTION

Continuous laser heating, pulsed laser heating, and continuous Joule heating in diamond anvil
cells have been used for a wide variety of melting, 1–3, synthesis, 4 and transport measurements 5,6
up to several 100s of GPa of pressure. Until very recently, pulsed Joule heating had not been
combined with DACs despite the long history of successful pulsed Joule heating at near-ambient
pressure, 7–11 the success of pulsed laser methods, 5,6,12 and finite element models suggesting it
could provide an unambiguous way to detect melting transitions. 13

In a 2021 paper, we showed that pulsed Joule heating at the μ s timescale can indeed be used to 29 generate melting data up to 110 GPa for platinum samples. 14 Melting was unambiguously and re-30 producibly identified by the plateau in temperature versus time during heating – a plateau caused 31 by the latent heat of fusion. In many cases, melting could be detected while maintaining sam-32 ples in a molten state for less than 10 µs, a five-order-of-magnitude decrease in duration com-33 ared to competing techniques such as X-ray absorption spectroscopy. 15 The experiments relied 34 on electrical pulses with ~ 10 A current amplitude and ~ 10 V voltage amplitude, values far be-35 ow the kA and kV amplitudes used in traditional "exploding wire experiments" at near-ambient 36 pressure. 7-9,14 Our electronics were based on a solid-state switch that was triggered directly from 37 delay generator. Moreover, the pulse amplifier was small, safe, and robust enough to transport to 38 synchrotron facility for X-ray measurements synchronized with the Joule heating pulses. 39

However, three limitations of the pulse amplifier and sensing circuitry were detected during the platinum melting experiments.¹⁴ First, the pulse power was limited by the 60 V maximum rating of the N-channel MOSFET used as the amplifier's primary switch. Second, at least one of the instrumentation amplifiers used for current and voltage sensing seemed to become damaged, causing spurious distortions in our final set of measurements (Section S1c of Ref. 14). Third, the accuracy of the sample resistance measurement deteriorated as resistance became smaller than the impedance of the low-side MOSFET plus electrical leads. The problem was that the common mode rejection ratio of the electrical sensing circuitry was too high to accurately measure small values of four-point-probe voltage. Finally, a fourth limitation is that we did not formally characterize the accuracy of resistance measurements before damaging the electronics.

Here, we describe a new pulse amplifier and electrical sensing equipment, which together improve upon all four limitations. First, the new amplifier has improved voltage range: 400 V instead of 60 V. Second, the electrical sensing equipment is much more robust, since it relies on passive

PLEASE CITE THIS ARTICLE AS DOI: 10.1063/5.0171213

probes. Third, the accuracy of voltage measurements for low resistance samples is improved be-53 cause of the new design that uses a high-side switch and passive probes. Finally, we document the 54 high accuracy of voltage and current measurements by presenting results for a 100 m Ω dummy 55 sample. In addition, we present proof-of-concept examples of resistance measurements during the 56 pulsed Joule heating of iron at pressures and temperatures up to ~ 150 GPa and 3200 K.

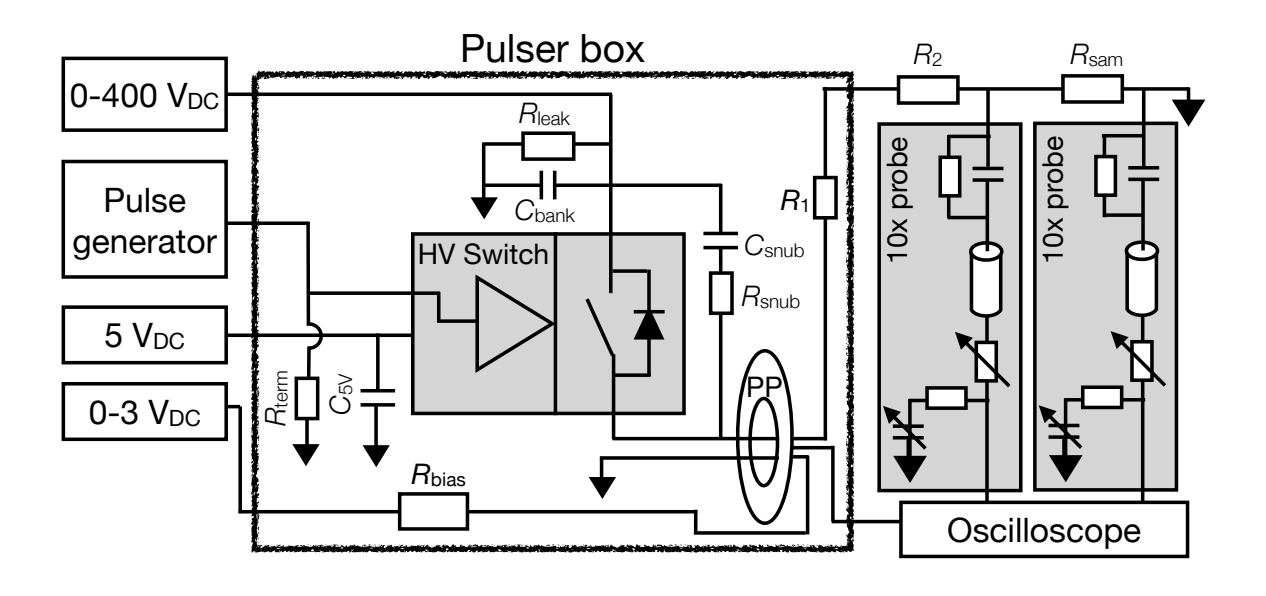


FIG. 1. Schematic of the pulse amplifier, current probe, and voltage probes. The large black box contains the electrical elements that are placed inside the metal enclosure. The shaded rectangles inside the pulse amplifier box shows the schematic of the Behkle high voltage switch. Voltage and current probes are marked by the shaded boxes labeled "10x probe" and the donut labeled "PP". Part numbers are listed in Table I.

ELECTRICAL DESIGN

The pulse amplifier is designed around the HTS-81-25-B switch from Behlke (Fig. 1). The 59 switch is powered by 5 V and 0.2 A from a regulated DC power supply. A DC power supply 60 charges the primary capacitor, " C_p ", which stores charge at the high voltage side of the switch. 61 We use voltages up to 400 V, a value below the primary capacitor's 500 V safety rating (Table 62 I). When the switch is triggered by a TTL signal (2-5 V amplitude) from a pulse generator, the capacitor is discharged through a series of buffer resistors and through the sample to ground. The first buffer resistor, R_1 , is a 1 Ω resistor that is hard-wired inside the pulse amplifier box. 65 The second buffer resistor, R_2 , is twisted into the delivery leads (Fig. 2d), allowing the user to

PLEASE CITE THIS ARTICLE AS DOI: 10.1063/5.0171213

(a) 2 cm (c) 10x probe 2 cm (e) (d)2 cm

FIG. 2. Photos and a schematic showing the physical arrangement of electronics during DAC experiments. (a) The front of the pulse amplifier. Several jacks were used for testing and are not used in this study. (b) The small circuit board that is used to connect the diamond cell to the electronics. (c) A schematic of the small circuit board and its electrical connections. Labels correspond to the labels in Fig. 1. (d) Three electrical leads. Each can be used to connect the pulse amplifier box to the sample. Two leads include resistors with $R_{\text{lead}} = 10$ or 3 Ω . (e) The pulse amplifier and diamond cell in action. The pulse amplifier rests sideways on an optical table. The diamond cell is held on a V-block between objective lenses. The small circuit board is screwed on to the diamond cell, and connected to the high pressure sample by thin wires that enter through the diamond cell portholes. Two 10x oscilloscope probes are connected to the small circuit board by SMA connectors.

2 cm

PLEASE CITE THIS ARTICLE AS DOI: 10.1063/5.0171213

85

90

91

easily switch between values of R_2 . The data presented here uses $R_2 = 0$ or 3 Ω . The discharge is cut off when the TTL signal ends. The natural decay timescale of the capacitor discharge is $\tau = RC = (R_1 + R_2 + R_{sam}) \times 70 \ \mu\text{F}$, which equals 70 μ s for $R_2 = 0 \ \Omega$ and 280 μ s for $R_2 = 3 \ \Omega$. In other words, the pulse current decays exponentially to the maximum current of the DC power supply in 100s of μ s.

Electrical sensing relies on three passive probes: a broadband current monitor (also known as a 72 'Pearson probe"; labeled "PP"), and two 10x oscilloscope probes. Part numbers are listed in Table 73 The Pearson probe outputs a voltage to the oscilloscope that is equal to 0.1 times the current. Hence, the oscilloscope measures 0.1I, $0.1V_+$, and $0.1V_-$, where V_+ and V_- are four point probe 75 voltages at the high side and low side of sample, respectively. (After collecting the data for this 76 manuscript, a third voltage probe was added to monitor voltage at the output of the pulse amplifier box, which is convenient for monitoring resistance in a two point probe configuration.) 78

Note that the use of a high-side switch enables the use of a passive voltage probe to measure 79 accurate values of $\Delta V = V_+ - V_-$. If we had used a low-side switch and passive voltage probes, 80 each probe would measure the voltage of interest plus the voltage drop across the switch, which 81 often much larger than the voltage of interest. For example, if the switch's series resistance is Ω and the high pressure metal sample's resistance is $\frac{1}{50}~\Omega=20~\text{m}\Omega,$ a 1% error in measurement of V_+ or V_- propagates to $\sim 50\%$ error in ΔV .

Two additional components help avoid saturation of the electrical measurements at high current and voltage. First, if the integral of current over time exceeds ~ 0.02 Amp-seconds for a single 86 pulse, Pearson probe Model 411 saturates according to the manufacturer's specification sheet. To extend the time-current integral for the highest current pulse presented here, we follow the manufacturer's recommendation to run 0.1 A of continuous direct current in the reverse direction through a very simple circuit that consists of a DC power supply and a 3 Ω resistor (" R_{bias} " in Fig. 1). Second, if the Pearson probe's output voltage exceeds the 50 V range of the oscilloscope, we add a 10 dB attenuator at the oscilloscope input. 92

Additional resistors and capacitors are added to the pulse amplifier to damp oscillations. A 93 47 Ω resistor labeled " R_{term} " in Fig. 1 terminates the output from the pulse generator. A 10 μ F capacitor buffers the 5 V DC power supply. A capacitor and resistor in series create a low-pass filter, which damps high frequency oscillations that would otherwise oscillate across the switch when it is turned on and off. They are labeled " $C_{\rm snub}$ " and " $R_{\rm snub}$ ". Their product, $R_{\rm snub}C_{\rm snub}=$ 97 $1\Omega \times 50 \ \mu\text{F} = 50 \text{ ns}$ is the low pass filter timescale.

PLEASE CITE THIS ARTICLE AS DOI: 10.1063/5.0171213

Finally, two features are added for safety purposes. First, a 250 k Ω resistor, " R_{leak} ", drains the 99 capacitor " C_p " in the characteristic time $R_{\text{leak}}C_p = 17$ seconds. Second, a panel-mount voltmeter 100 monitors the voltage on the high side of the capacitor. The voltmeter is shown in the photo in Fig. 101 2a, but not in the schematic. 102

III. MECHANICAL DESIGN AND CONSTRUCTION 103

A $25 \times 20 \times 13$ cm metal box houses a circuit board that is held on four standoffs. Five elements 104 are attached by screws to the circuit board: the Pearson probe, the HV switch, and three power 105 resistors (R_{leak} , R_{bias} and R_1). The primary capacitor, C_p , is pressed into through holes and soldered. 106 The other elements are attached by solder. The faces of the box hold the panel-mount voltmeter, 107 panel-mount BNC connectors for connections with the DC power supplies, pulse generator, and 108 oscilloscope, and a panel-mount barrel connector that connects to $R_{\rm lead}$ and $R_{\rm sam}$ to the pulse 109 amplifier. The oscilloscope probes are fastened onto a face of the box for strain relief. 110

A small circuit board is attached to the body of each diamond anvil cell in order to provide 111 strain relief for the electrical connections (Fig. 2). Electrical breakdown (i.e. arcing) is not a 112 problem on either board as long as the gaps between high and low voltage regions are greater than 113 0.2 mm. We typically use 2 mm-wide gaps, corresponding to an electrical breakdown voltage in 114 air of 2 mm \times 3 kV/mm = 6 kV, which is far larger than the 400 V maximum voltage we use. The copper clad board itself is rated to 40 kV. 16

RESULTS 117

121

122

123

124

125

100 m Ω dummy sample 118

The pulse amplifier is tested with $R_{\text{sam}} = 100 \text{ m}\Omega$ and $R_2 = 0 \text{ or } 3 \Omega$. The 100 m Ω dummy 119 sample is Ohmite brand, part number WHER10FET. It has a nominal precision of 1% in resistance, 120 which we confirm by measurement with a Keithley Sourcemeter 2400 before and after pulsing high amplitude currents through it. It has a power rating of 5 W, which seems to be sufficient for all pulses tested here, even when peak power reaches 4 kW in our highest amplitude pulses. If the resistor's temperature had increased due to Joule heating, we would expect to measure a steady increase in resistance during a pulse; we detected no such increase. Single pulses are used during 100 m Ω dummy testing (i.e. no averaging to reduce noise). The start and end of each pulse is

PLEASE CITE THIS ARTICLE AS DOI: 10.1063/5.0171213

127

128

129

130

131

132

133

134

135

136

137

138

139

140

141

142

143

144

(a) (b) (c) 0.11 Resistance (Ω) 0 Current (A) /oltage (V) Voltage (V) 5 0.10 V-0.09 0 5 0 5 5 0 Time (µs) Time (µs) Time (μ s)

FIG. 3. A 5 μ s pulse to 60 A through the 100 m Ω dummy sample. (a) Voltage measurements from electrodes that probe just above and just below the dummy sample in a four point configuration. (b) Current measured by the Pearson probe (blue) and four point probe voltage (red) calculated by the difference between curves in (a). (c) Pulsed resistance measurement (black) and actual 100 m Ω resistance (cyan line) with ± 5 %error envelope (cyan shading). Settings: $R_2 = 3 \Omega$, SRS power supply, 0 A through R_{bias} .

triggered by a pulse generator (Berkeley Nucleonics Model 525).

An example of a 5 μ s pulse using $R_2 = 3 \Omega$ is shown in Fig. 3. The current rises to $I_{\text{max}} = 60 \text{ A}$ with a rise time of 460 μ s, and drops to 0 A with a fall time of 350 μ s. Rise time and fall time are defined by time interval between $10\% I_{\text{max}}$ and $90\% I_{\text{max}}$. Resistance is determined by dividing the four point probe voltage by current. In this example, the accuracy of resistance is better than 5% at all times from 1.4 to 4.9 μ s.

Prior to 1.4 μ s, the resistance measurement is higher than the known 100 m Ω value, likely due to the self-inductance of the dummy sample. Indeed, the ~ 1.3 V excess voltage measured at = 0.7 μ s in Fig. 3b can be explained by induced voltage, $L\frac{dI}{dt}$, for the measured rate of change of current, $\frac{dI}{dt} = \frac{50}{0.6}$ A/ μ s, and the inductance, L = 16 nH, which is equal to the theoretical value of self-inductance of a 2.1 cm-long, 1 mm-diameter piece of straight wire. 17 The excess negative voltage measured during the pulse turn off at $\sim 5.7 \,\mu s$ can be explained in the analogous way.

Fig. 4 shows four other tests that demonstrate the range of pulses that can be driven from the pulse amplifier. The pulse amplifier can operate over three orders of magnitude in pulse duration and in peak current: 5 μ s to 10 ms, and 0.2 to 200 A. In almost all cases, resistance measurements are within 5% of the true value at all times from $\sim 2 \,\mu s$ until the end of the pulse (Fig. 4b,f,h). The main exception is that the error reaches $\sim 6\%$ during the highest amplitude pulse (Fig. 4d). Note that to achieve the longest pulses, we used a high current DC power supply (XANTREX XHR 60-18), whereas to achieve relatively short, high voltage pulses we used an SRS PS310 power

PLEASE CITE THIS ARTICLE AS DOI: 10.1063/5.0171213

160

161

The longest duration pulse that can be measured with high accuracy in our measurement scheme 151 is 10 ms. At longer times, Pearson probe Model 411 approaches its low frequency bandwidth limit. The manufacturer's specification sheet lists a 0.9 %/ms "droop rate", and indeed at 10s 153 of ms, the measured current decreases steadily over time by more than 10% even though the 154 voltage measurement remains steady. Numerical correction for the droop rate might be possible if 155 a calibration of droop rate were performed.

Using $R_2 = 0 \Omega$, the rise time is 1 μ s. Using $R_2 = 3 \Omega$, a faster rise time of ~ 500 ns is achieved 157 (Figs. 4a,c). Further increasing R_2 to 10 or 25 Ω has no effect on the rise time. The rise time is also 158 sensitive the snubber components (C_{snub} , R_{snub}). By choosing a smaller values of C_{snub} or R_{snub} , 159 the rise time increases by a small amount, but the stability of the pulse amplifier is reduced. For example, decreasing $C_{\rm snub}$ to 25 nF reduces the rise time to \sim 350 ns, but the rising edge of the pulse includes a few oscillations. For $C_{\text{snub}} = 10$ nF, the oscillation amplitude increases further 162 for both the rising edge and the falling edge, and the sharpness of the rising edge is essentially 163 unchanged. 164

This is the author's peer reviewed, accepted manuscript. However, the online version of record will be different from this version once it has been copyedited and typeset. PLEASE CITE THIS ARTICLE AS DOI: 10.1063/5.0171213

(a) (b) 0.11 Resistance (Ω) Current (A) Voltage (V) 0.09 5 ò 5 Time (µs) Time (µs) (c) 0.11 Resistance (Ω) 0.25 (A) 0.00 Current 0.25 (A) Voltage (V) 0.25 0.00 0.000 0.09 0 5 0 Time (µs) Time (µs) (e) 0.11 Resistance (Ω) Current (A) Voltage (V) 0.09 200 200 Time (µs) Time (µs) (g) 0.11 Resistance (Ω) Current (A) Voltage (V) 0.1 10 0.09 10 Time (ms) Time (ms) (j) Resistance (Ω) Current (A) Voltage (V) 20 0.09 10 0 10 0 Time (ms)

FIG. 4. Five pulses through the $100 \text{ m}\Omega$ dummy sample. Each row shows the four point probe voltage (red), current (blue), and resistance (black). (a,b) A 5 μ s pulse to 35 A using $R_2 = 0 \Omega$ and the SRS power supply. (c,d) A 5 μ s pulse to 0.2 A using $R_2 = 3 \Omega$ and the SRS power supply. (e,f) A 250 μ s pulse peaking at 200 A using $R_2 = 0 \Omega$, the SRS power supply at 400 V, and 0.1 A DC current through R_{bias} . (g,h) A 10 ms pulse to 0.14 A using the $R_2 = 3 \Omega$ and the XHR power supply. (j,i) A 10 ms pulse to 18 A using $R_2 = 0 \Omega$ and the XHR power supply. Time series in rows 3, 4, and 5 are filtered with Savitkzy-Golay filters with polynomial order 2 and 10, 30, and 10 μ s timescale, respectively.

Iron sample at high pressure

165

166

167

168

We demonstrate the utility of the pulse amplifier by using it to heat one sample of iron compressed statically to 77 ± 2 GPa at room temperature, and another sample of iron compressed statically to \sim 125 GPa. Pressure was measured before and after heating using the diamond Ra-

PLEASE CITE THIS ARTICLE AS DOI: 10.1063/5.0171213

FIG. 5. (a) Two photographs overlaid: a white light image of a piece of iron compressed to 77 GPa in a diamond anvil cell, and a image of the same piece of iron being heated by 500 repetitions of 5 μ s-long electrical pulses. The orange glow is the thermal emissions from the heated sample. "V+" and "V-" mark the voltage probes. "I+" and "I-" mark the electrodes that deliver current. (b) Current during five sets of 500 pulses, each of which uses a driving voltage from 5 to 19 V. (c) Four point probe voltage during the same sets of pulses. (d) Resistance during the same sets of pulses. Colors in (b) and (c) mark the data used to infer resistance in (d).

PLEASE CITE THIS ARTICLE AS DOI: 10.1063/5.0171213

man edge. 18 The iron sample is shaped into a four point probe geometry and compressed between layers of KCl insulation in the sample chamber of a diamond anvil cell using 200 µm culets. See 170 Ref. 19 for details of sample fabrication and preparation. The starting thickness of each layer (top 171 insulation, bottom insulation, and iron sample) is $\sim 10 \ \mu m$ for the 77 GPa sample, and $\sim 5 \ \mu m$ 172 for the 125 GPa sample. 173

We heat the 77 GPa iron sample with 5 μ s pulses of current. At pulse amplitudes > 5 A, a 174 region of the surface of the sample visibly heats up, as evidenced by the orange glow in Fig. 5a. 175 The color temperature of light emitted from a 5 μ m-disc centered on the hotspot is ~ 2000 K; see 176 Ref. 20 for details of the spectroradiometric temperature measurements.

Examples of pulsed heating at 77 GPa are shown in Figs 5b-d. At low current amplitude, 178 the resistance is steady. At higher current amplitudes, the resistance increases more than 3-fold 179 during the pulse as the sample heats to 1000s of K. One example of heating the 125 GPa sample 180 is shown in Fig. 6. The sample temperature and pressure peak at ~ 3200 K and ~ 150 GPa. 181 Thermal pressure of the 125 GPa sample is estimated based on the thermal equation of state of 182 iron, assuming an isochoric heating trajectory.²¹

DISCUSSION

To summarize the wide range of pulses described above, we overlay many pulses in a log-log 185 plot (Fig. 7). 186

To give ideas of how the pulse amplifier can be used, we describe pulses in relationship to a 187 "prototypical pulse" for diamond cell experiments, which we define as the pulse plotted in yellow 188 in Fig. 7. It is a 5 μ s pulse that peaks at \sim 8 A and causes the 77 GPa iron sample glow orange. 189 The pulse amplitude can be decreased 40-fold to 0.2 A, a change that can be useful to avoid heating 190 a sample while measuring its resistance. The pulse amplitude can be increased 7-fold to 60 A, or 191 lengthened 200-fold to 10 ms, changes which are crucial for heating thicker or wider samples. 192

If a decaying pulse shape is acceptable, the prototypical 8 A pulse can be increased 25-fold 193 to 200 A. This pulse is useful to melt relatively thick samples at low pressure. For example, we 194 used a pulse with $I_{\text{peak}} = 70 \text{ A}$ and $100 \mu \text{s}$ duration to melt an ambient pressure iridium sample 195 described in Ref. 20. 196

Shorter duration pulses are possible by triggering the switch with TTL signals that are shorter 197 than 5 μ s. As duration decreases, several issues arise. First, at $\sim 2 \mu$ s pulse duration, the plot of

PLEASE CITE THIS ARTICLE AS DOI: 10.1063/5.0171213

current-versus-time is rounded, not square, because the current rise and fall begin to overlap, at 199 least for the $\sim 100 \,\mathrm{m}\Omega$ dummy sample. At 1 μ s pulse duration, the error in resistance measurement 200 becomes huge (> 100%), likely due to inductance of the sample and current-carrying electrodes.²² 201 To correct for the inductance spikes, the method proposed in Ref. 22 could be useful. For trigger 202 durations shorter than 1 μ s, the pulse amplifier fails to turn on completely, because the rise time 203 and fall time of the drive circuitry is too slow. We attempted to decrease the rise and fall times 204 substantially by decreasing $R_{\rm snub}$ and/or $C_{\rm snub}$ by 2-fold and 5-fold, but with no success. The rise 205 time remained > 300 ns. In addition, the rising edge begins to oscillate at low values of $R_{\rm snub}C_{\rm snub}$. 206 The ~ 300 ns lower limit for the rise time is surprising, because the Behlke switch has a nominal 207 rise time of ~ 10 ns. Albeit, we use much lower current and voltage than any of the test results 208 reported on the manufacturer's specification sheet ($\geq 25 \text{ A}, \geq 840 \text{ V}$). 209

To reach even shorter pulse times, vacuum tube technology may be useful, following the elec-210 trical designs in pioneering near-ambient pressure studies.^{7–11} At near-ambient pressures, pulse 211 amplifiers are almost always based on vacuum tube technologies such as triggered spark gaps or 212 ignitrons because of their high current and voltage ratings (> kA, kV).²³ Typically, two spark 213 gaps are used: one to start the pulse and a second one to end the pulse. Two are required because 214 spark gaps are "semi-controlled" switches, meaning they can only be externally controlled in one 215 direction, on or off. Unfortunately, each spark gap requires a high voltage (~kV) trigger, which 216 typically provided by yet another vacuum tube (e.g. a thyratron), adding complexity to the circuit. 10,11 In contrast, we control the Behkle switch with a single TTL-level pulse.

CONCLUSIONS

A broadband pulse amplifier has been built and characterized. It can heat metals in diamond 220 anvil cells up to at least 150 GPa and 3200 K. The pulse amplifier delivers 0.2 to 200 A with pulse 221 durations in the range 5 μ s – 10 ms. When coupled with passive current and voltage probes, the 222 accuracy of the typical four point probe resistance measurement is better than 5%. The new pulse 223 amplifier provides a more reliable and more versatile substitute for the amplifier used previously 224 for pulsed Joule heating experiments up to ~ 110 GPa and 4500 K.¹⁴

This is the author's peer reviewed, accepted manuscript. However, the online version of record will be different from this version once it has been copyedited and typeset. PLEASE CITE THIS ARTICLE AS DOI: 10.1063/5.0171213

226 ACKNOWLEDGMENTS

- This material is based upon work supported by the National Science Foundation under Grant
- No. 2125954. We thank Seth Wagner for machining parts. We thank Maddury Somayazulu for
- 229 fruitful discussions.

230 DATA AVAILABILITY STATEMENT

The data that support the findings of this study are available at 10.5281/zenodo.10138973.²⁴

(b) Current (A) 6 2 Z Time (μs) 0 4 (c) 1.0 Voltage (V) PLEASE CITE THIS ARTICLE AS DOI: 10.1063/5.0171213 0.0 6 0 2 4 (d) Time (µs) Resistance (Ω) 0.05 2.5 3.0 3.5 4.0 2.0 Time (µs)

(a)

FIG. 6. A sample of iron pulsed compressed statically to \sim 125 GPa, and pulsed Joule heated to \sim 3200 K and ~ 150 GPa. (a) Two photographs overlaid: a white light image of a piece of iron at room temperature, and a image of the same piece of iron being heated by ten repetitions of 4 μ s-long electrical pulses. The white glow at the center of the image is the thermal emissions from the heated sample. White lines are annotations that mark the edges of the metal sample and electrodes. (b) Current during ten pulses using a driving voltage of 13 V. (c) Four point probe voltage. (d) Resistance. Black curves in (b) and (c) mark the data used to infer resistance in (d).

PLEASE CITE THIS ARTICLE AS DOI: 10.1063/5.0171213

10³ 10^{2} Current (A) 10^{1} 10⁰ −1 L 10 10-4 10^{-6} 10⁻³ 10^{-2} 10 Time (s)

FIG. 7. Current versus time with log scaling for all data shown in Figs. 3, 4, 5, 6. Blue curves show the current pulses through the $100 \text{ m}\Omega$ dummy sample. Black, brown, red, orange, and yellow curves show the current pulses through the 77 GPa iron sample. The grey curve shows the current pulse used to heat the 125 GPa iron sample. Data is truncated for clarity. For example, the long duration pulses are truncated at times shorter than the time-resolution of the data.

This is the author's peer reviewed, accepted manuscript. However, the online version of record will be different from this version once it has been copyedited and typeset.

PLEASE CITE THIS ARTICLE AS DOI: 10.1063/5.0171213

TABLE I. List of parts and specifications. Not included: metal casing, connectors, cables, circuit board, panel-mount voltmeter.

| Label | Specifications | | Brand and part number |
|--------------------------|-----------------------|------------------------|-----------------------|
| Oscilloscope | 200 MHz | 4 channels | Picoscope 5444D |
| Pulse Generator | 50 MHz | TTL | BNC 525 |
| HV supply (option 1) | 1250 V | 20 mA | SRS PS310 |
| HV supply (option 2) | 60 V | 18 A | XANTREX XHR 60-18 |
| HV Switch | 250 A _{peak} | 8.4 kV | Behlke HTS-81-25-B |
| PP | 20 MHz | 5000 A _{peak} | Pearson 411 |
| DC supply | 30 V | 5 A | Madell TPR3003 |
| 10x Probe | 400 MHz | 4 meters | Probemaster 6143-4 |
| C_p | $70~\mu \mathrm{F}$ | 500 V | TDK B32758G2706K000 |
| $C_{ m snub}$ | 50 nF | 500 V | |
| $R_{ m bias}$ | 3 Ω | 50 W | Ohmite 850F3R0E |
| R_1 | 1 Ω | 10 W | Ohmite 810F1R0E |
| R_{leak} | $250~k\Omega$ | 50 W | Ohmite L50J250KE |
| R_{sam} (dummy) | 0.1 Ω | 5 W | Ohmite WHER10FET |
| $C_{5 m V}$ | $10~\mu { m F}$ | 25 V | Nichicon UPS1E100MDD |
| $R_{ m term}$ | 47 Ω | 1/4 W | Ohmite OD470JE |
| $R_{ m snub}$ | 1 Ω | 1/2 W | |

accepted manuscript. However, the online version of record will be different from this version once it has been copyedited and typeset is the author's peer reviewed,

PLEASE CITE THIS ARTICLE AS DOI: 10.1063/5.0171213

REFERENCES

- ¹S. T. Weir, M. J. Lipp, S. Falabella, G. Samudrala, and Y. K. Vohra, Journal of Applied Physics
- **111**, 123529-123529-5 (2012).
- ²R. Sinmyo, K. Hirose, and Y. Ohishi, Earth Planet. Sci. Lett. **510**, 45 (2019).
- ³P. Parisiades, Crystals **11** (2021), 10.3390/cryst11040416.
- ⁴M. E. Alabdulkarim, W. D. Maxwell, V. Thapliyal, and J. L. Maxwell, Journal of Manufacturing
- ²³⁸ and Materials Processing **7** (2023), 10.3390/jmmp7020057.
- ⁵T. Yagi, K. Ohta, K. Kobayashi, N. Taketoshi, K. Hirose, and T. Baba, Measurement Science
- and Technology **22**, 024011 (2011).
- ⁶Z. Konôpková, R. S. McWilliams, N. Gómez-Pérez, and A. F. Goncharov, Nature **534**, 99
- 242 (2016).
- ⁷C. Cagran and G. Pottlacher, in *Handbook of Thermal Analysis and Calorimetry Recent Ad-*
- vances, Techniques, and Applications, Vol. 5, edited by M. E. Brown and P. K. Gallagher (Else-
- vier, 2008) 5th ed., Chap. 9, pp. 299–320.
- ⁸A. Cezairliyan and J. L. McClure, Int. J. Thermophys. **8**, 577 (1987).
- ⁹A. M. Kondratyev and A. D. Rakhel, Phys. Rev. Lett. **122**, 175702 (2019).
- ¹⁰R. Gallob, H. Jäger, and G. Pottlacher, Int. J. Thermophys. **7**, 139 (1986).
- ²⁴⁹ ¹¹K. W. Henry, D. R. Stephens, D. J. Steinberg, and E. B. Royce, Review of Scientific Instruments ²⁵⁰ **43**, 1777 (1972).
- ¹²M. Zaghoo, A. Salamat, and I. F. Silvera, Phys. Rev. B **93**, 155128 (2016).
- ²⁵² ¹³Z. M. Geballe and R. Jeanloz, J. Appl. Phys. **111**, 123518-123518-15 (2012).
- ¹⁴Z. M. Geballe, N. Holtgrewe, A. Karandikar, E. Greenberg, V. B. Prakapenka, and A. F. Gon-
- charov, Phys. Rev. Materials **5**, 033803 (2021).
- ¹⁵S. Boccato, R. Torchio, S. Anzellini, E. Boulard, F. Guyot, T. Irifune, M. Harmand, I. Kantor,
- F. Miozzi, P. Parisiades, A. D. Rosa, D. Antonangeli, and G. Morard, Scientific Reports 10
- 257 (2020), 10.1038/s41598-020-68244-3.
- ¹⁶Https://www.mgchemicals.com/downloads/tds/tds-500-series.pdf.
- ¹⁷E. B. Rosa, *The self and mutual inductances of linear conductors*, 80 (US Department of Com-
- merce and Labor, Bureau of Standards, 1908).
- ¹⁸Y. Akahama and H. Kawamura, Journal of Applied Physics **100**, 043516-043516-4 (2006).

PLEASE CITE THIS ARTICLE AS DOI: 10.1063/5.0171213

- ¹⁹Z. M. Geballe, S. M. Vitale, J. Yang, F. Miozzi, V. V. Dobrosavljevic, and M. J. Walter, "A
- diamond anvil microassembly for joule heating and electrical measurements up to 150 gpa and 263
- 4000 k," (2023), arXiv:2310.18176 [physics.app-ph]. 264
- ²⁰Z. M. Geballe, F. Miozzi, C. F. Anto, J. Rojas, J. Yang, and M. J. Walter, "Spectroradiome-265
- try with sub-microsecond time resolution using multianode photomultiplier tube assemblies," 266
- (2023), arXiv:2310.16660 [physics.ins-det]. 267
- ²¹F. Miozzi, J. Matas, N. Guignot, J. Badro, J. Siebert, and G. Fiquet, Minerals **10**, 100 (2020).
- ²²E. Kaschnitz, G. Pottlacher, and H. Jäger, International Journal of Thermophysics 13, 699 269
- (1992).270
- ²³E. Cook, in *Linac* 2000, edited by A. W. Chao (2000) p. 663, arXiv:physics/0008189 271
- [physics.acc-ph]. 272
- ²⁴Z. Geballe, J. Lai, and M. Walter, "Zenodo data: A broadband pulse amplifier for Joule heating 273
- experiments in diamond anvil cells," (2023). 274